AIAA JOURNAL
Vol. 36, No. 1, January 1998

Progressive Failure Analysis of Pin-Loaded Laminated Composites Using Penalty Finite Element Method

Seung Jo Kim* and Joon Seok Hwang†
Seoul National University, Seoul 151-742, Republic of Korea
and
Jin Hee Kim‡
Korea Aerospace Research Institute, Taejon 305-600, Republic of Korea

A progressive failure analysis is carried out to predict the failure strengths and failure modes of pin-loaded laminated composite plates using the penalty finite element method. To consider contact condition in the pin hole interface, an exterior penalty method and the Coulomb friction law are used. Damage accumulations in the laminates are evaluated by using Hashin's failure criteria combined with the proposed property degradation model. Using a finite element code developed based on the present formulation, contact stresses are obtained and verified. Predictions of failure strengths and the failure modes compare well with available experimental data. Finally, a parametric study considering geometries and clearance is performed to identify the failure characteristics of the pin-loaded laminated composite plate. The numerical results show the importance of geometric parameters and clearance on both the failure strengths and the failure modes.

Nomenclature

$\boldsymbol{B}$	= strain–displacement interpolation matrix
$\boldsymbol{C}$	= anisotropic elasticity tensor or stiffness matrix
D	= diameter of the hole
E	= distance from the upper edge to the center of the hole
$\boldsymbol{E}$	= differentiation matrix
$\boldsymbol{F}$	= force vector
$\boldsymbol{f}$	= body force
$\boldsymbol{H}$	= displacement interpolation matrix
$\boldsymbol{K}$	= global stiffness matrix
L	= length of the plate
$\boldsymbol{n}$	= normal vector
P	= applied load
R, R_h	= radius of hole
R_p	= radius of pin
S	= average bearing stress, $S = P/Dt$
s	= contact clearance between the pin and the hole
t	= thickness of the plate
$\boldsymbol{t}$	= traction force
$\boldsymbol{U}$	= global displacement vector
W	= width of the plate
Γ_C	= candidate contact boundary
Γ_D	= displacement prescribed boundary
Γ_F	= force prescribed boundary
ε	= penalty parameter
$\boldsymbol{\varepsilon}$	= strain tensor
λ	= nondimensionalized contact clearance, $(R_h - R_p)/R_h$
μ	= friction coefficient
$\boldsymbol{\sigma}$	= stress tensor
$\sigma_N(\tau_r)$	= normal contact stress
$\sigma_T(\tau_{r\theta})$	= frictional stress on the contact boundary
Ω	= domain of the plate with pin hole

Introduction

PIN-LOADED joints in laminated composite structures are commonly used in aerospace vehicles. But the laminated composite plates with a pin joint have somewhat weak points due to its brittle nature, unlike those in the conventional metals, such as aluminum and titanium. Furthermore, the stress concentrations are more severe than those of the conventional metals in the area around the pin–hole interface. Therefore, a deep understanding of strengths and failure modes is very important to provide reliable design of pin-loaded joints in laminated composite structures.

Several analyses have been performed for predicting the failure strengths and failure modes of pin-loaded laminated composite plates.[1–12] Among them, several studies were performed by assuming a known cosinusoidal radial traction around the hole or by assuming a known contact area.[1,4,5,9–11] Although this assumption has been admitted as a permissible approximation for isotropic materials, the load distribution around the hole is far different from cosinusoidal distribution with the variation of ply orientation in laminated composite plates.[13,14] Also, only a few works consider frictional effect.[2,3,8,12] In addition, the failure in the pin-loaded structures happens in a progressive manner.[9] The contact stresses change with the degree of material deterioration of laminated composite plates. Therefore, an analysis considering both the progressive failure mechanism and varying contact stresses is necessary. But, until now, such an analysis has not been performed for the failure analysis of pin-loaded laminated composite plates.

In this paper the failure strengths and the failure modes of pin-loaded laminated composite plates are analyzed based on the progressive failure concept and the penalty finite element method. To impose contact condition between the pin and the hole, the exterior penalty method[15] and the Coulomb friction law[16,17] are used. Hashin's failure criterion,[18] which can predict the fiber mode failure and the matrix mode failure separately, is used to predict the lamina failure. The ply discount method[19] with the proposed property degradation model is taken to simulate the stiffness degradation in each ply. Using the developed finite element code, the contact stresses around the pin–hole interface are compared with existing works.[13,14] Also, the comparison of the failure strength and the failure modes between the present results and the available experimental results is performed. Finally, the parametric studies are carried out to identify the characteristics of the pin-loaded joint.

Description of the Problem

Let us consider a laminated composite plate containing a single pin hole as shown in Fig. 1. The plate has the dimensions of length L, width W, and thickness t. The uniform loading P is applied to the lower edge of the plate, and the following general assumptions are made for simplifying the problem.

Received Dec. 4, 1996; revision received Sept. 5, 1997; accepted for publication Sept. 23, 1997. Copyright © 1997 by the American Institute of Aeronautics and Astronautics, Inc. All rights reserved.

*Professor, Department of Aerospace Engineering. Member AIAA.
†Graduate Research Assistant, Department of Aerospace Engineering.
‡Senior Researcher, Space Division, P.O. Box 113, Yusong. Member AIAA.

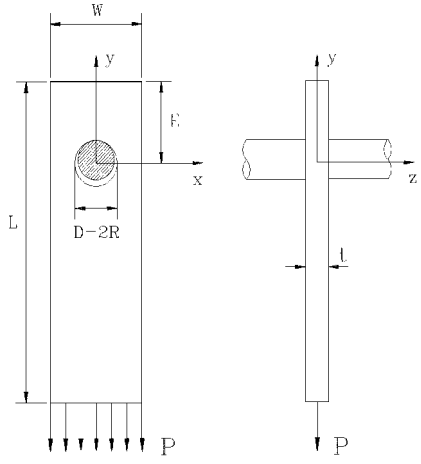

Fig. 1 Configurations of a pin-loaded laminated composite plate.

1) The pin is rigid.
2) Laminated composite plates have symmetric stacking sequences.
3) Friction coefficient μ is constant on the pin–hole interface.
4) Linear elasticity holds.
5) The width and the length of the plate are considerably larger than its thickness; the plane stress assumption holds.
6) Perfect bondage exists between the plies in the laminated composite plate.

Theory

Variational Formulation

The pin-loaded joint problem can be stated as a general class of the contact problem. This problem is characterized by the following sets of equations and inequalities:

$$\sigma_{ij,j} + f_i = 0 \qquad \text{in} \qquad \Omega \tag{1}$$

$$u_i = 0 \qquad \text{on} \qquad \Gamma_D \tag{2}$$

$$\sigma_{ij} n_j = t_i \qquad \text{on} \qquad \Gamma_F \tag{3}$$

And on Γ_C, if $u_i n_i - s < 0$,

$$\sigma_N = 0, \qquad \sigma_T = 0 \tag{4}$$

and if $u_i n_i - s = 0$,

$$\sigma_{ij} n_i n_j < 0, \qquad |\sigma_T| = \mu |\sigma_N| \tag{5}$$

These systems of equations and inequalities describe the Signorini problem, which obeys the Coulomb friction law. It is generally accepted that there are two distinct regions, the slip region and the nonslip region, in the contact area when the frictional effect is considered. Within the scope of this work, all the contact region is assumed as the slip region because the portion of the nonslip region is very small at the low level of friction for most cases.[14] The strain–displacement relations are as follows:

$$\varepsilon = \tfrac{1}{2}\left[\nabla u + (\nabla u)^T\right] \tag{6}$$

And the stress–strain relation takes the following form by using the linear anisotropic elastic tensor C:

$$\sigma = C{:}\varepsilon \tag{7}$$

To solve these systems of equations and inequalities due to the unilateral contact, we use the exterior penalty method.[15] It is well known that the penalty method has several merits over other methods to solve the constrained problem, such as the contact problem.[14] The exterior penalty method has a simpler form for the finite element formulation compared with other penalty methods, such as the interior penalty and the extended interior penalty method. The exterior penalty method has few variables compared with the Lagrangian multiplier methods.

Using the principle of virtual work and the exterior penalty method, the preceding equations and inequalities can be described in the following variational form:

$$-\int_\Omega (\sigma_{ij,j} + f_i)\delta u_i \, dV + \int_{\Gamma_F} (\sigma_{ij} n_j - \overline{t_i})\delta u_i \, ds + \int_{\Gamma_C} (\sigma_{Ti} - \overline{\sigma_{Ti}})\delta u_i \, ds + \frac{1}{\varepsilon}\int_{\Gamma_C} (u_i n_i - s)^+ n_j \delta u_j \, ds = 0 \tag{8}$$

where

$$(f)^+ = \begin{cases} f & f > 0 \\ 0 & f \le 0 \end{cases} \tag{9}$$

Neglecting the body force and applying the divergence theorem to the first term, the following form is obtained:

$$\int_\Omega \sigma_{ij}\delta\varepsilon_{ij} \, dV - \int_{\Gamma_F} \overline{t_i}\delta u_i \, ds - \int_{\Gamma_C} \overline{\sigma_{Ti}}\delta u_i \, ds + \frac{1}{\varepsilon}\int_{\Gamma_C} (u_i n_i - s)^+ n_j \delta u_j \, ds = 0 \tag{10}$$

In general, it is very difficult to solve the frictional contact problem with two unknowns, the normal contact stress and the frictional stress, as pointed out by previous works.[20] Especially when the normal contact stress is prescribed on the contact area, the existence of the solution has been proved.[20] Therefore, the special solution procedures using the aforementioned existence of the solution are used in this paper in a manner similar to the previous works.[14,21] Unlike previous works, the friction force is calculated in a simple manner because we assume only the slip region in all the contact area.

Lamination Theory

Assuming the plane stress state, the stiffness of a laminated composite plate can be calculated by averaging the stiffness of each ply through the thickness of the plate. Therefore, the stiffness matrix of the plate can be described as follows. Let c_i be the ply stiffness matrix with respect to the global coordinate[22]:

$$C = \frac{1}{t}\sum_{i=0}^{N} t_i c_i \tag{11}$$

where

N = number of plies
t_i = thickness of ith ply

Under the perfect bondage assumption, the behavior of each ply is identical to that of the plate. Therefore, the stress state of each ply can be calculated using the global strain components.

Failure Analysis

It is a well-known fact that there are three basic failure modes in a pin-loaded joint in a laminated composite: the tension mode, the shear-out mode, and the bearing mode.[5,6]

Tension failure and shear-out failure are due to the tensile and shear stress concentration at the edge of the hole, respectively. Bearing failure is due to the high compressive stress on the loaded side of the hole. These failure modes are strongly related to the failure characteristics of the laminated composite itself. Within the scope of this paper, two failure mechanisms (fiber breakage and matrix cracking) are considered as the major failure mechanisms of laminated composites.

There are several failure criteria developed by many researchers.[18,23,24] Among them, Hashin's failure criterion[18] is widely used for the progressive failure analysis because this criterion can predict the fiber breakage and the matrix cracking mode separately. It is very important to identify the failure characteristic of laminated composites properly. Therefore, Hashin's failure criterion is selected in this paper.

Hashin's Failure Criterion

In the plane stress state, Hashin's failure criterion can be stated as follows with respect to the material coordinate (x_1 is along the fiber direction and x_2 is perpendicular to the x_1 axis).

Tensile fiber mode ($\sigma_{11} > 0$):

$$\left(\sigma_{11}/\sigma_A^+\right)^2 + (\sigma_{12}/\tau_A)^2 = 1 \tag{12}$$

Compressive fiber mode ($\sigma_{11} < 0$):

$$\sigma_{11} = -\sigma_A^- \tag{13}$$

Tensile matrix mode ($\sigma_{22} > 0$):

$$\left(\sigma_{22}/\sigma_T^+\right)^2 + (\sigma_{12}/\tau_A)^2 = 1 \tag{14}$$

Compressive matrix mode ($\sigma_{22} < 0$):

$$\left(\sigma_{22}/\sigma_T^-\right)\left[\left(\sigma_T^-/2\tau_T\right)^2 - 1\right] + (\sigma_{22}/2\tau_T)^2 + (\sigma_{12}/\tau_A)^2 = 1 \tag{15}$$

where

σ_A^+ = longitudinal tensile strength
σ_A^- = longitudinal compressive strength
σ_T^+ = transverse tensile strength
σ_T^- = transverse compressive strength
τ_A = longitudinal shear strength
τ_T = transverse shear strength

Property Degradation Model

Once the failure takes place in laminated composites, the material properties in the failed area degrade. The degree of property degradation is strongly related to the failure mechanism of laminated composites. According to the failure characteristics, the way in which the materials are damaged is very different. Also, when the loads are applied to the laminated composites, each ply behaves differently according to the stress state in itself, and so the failure mechanisms in each ply are different.

Therefore, the property degradation must be considered according to each failure mechanism in each ply. The property degradation models used in this work are as follows. Let c_{ij} be the material stiffness matrix with respect to the material coordinate of the lamina in the plane stress state.[22]

If fiber breakage occurs, make $\sigma_1 = 0$ irrespective of the strain state:

$$\begin{bmatrix} c_{11} & c_{12} & 0 \\ c_{12} & c_{22} & 0 \\ 0 & 0 & c_{66} \end{bmatrix} \Rightarrow \begin{bmatrix} 0 & 0 & 0 \\ 0 & c_{22} & 0 \\ 0 & 0 & c_{66} \end{bmatrix} \tag{16}$$

If matrix cracking occurs, make $\sigma_2 = \sigma_{12} = 0$ irrespective of the strain state:

$$\begin{bmatrix} c_{11} & c_{12} & 0 \\ c_{12} & c_{22} & 0 \\ 0 & 0 & c_{66} \end{bmatrix} \Rightarrow \begin{bmatrix} c_{11} & 0 & 0 \\ 0 & 0 & 0 \\ 0 & 0 & 0 \end{bmatrix} \tag{17}$$

These property degradation models are constructed in a manner similar to Lee's work.[19] But a modification is made because Lee's model may overestimate the lamina failure. Unlike Lee's model, which eliminates all of the stiffness terms in the case of fiber breakage, the present model eliminates only c_{11} and c_{12}.

Numerical Procedure

Finite Element Formulation

Following the usual two-dimensional finite element procedure, the displacement field is interpolated and then the strain field becomes

$$\begin{bmatrix} u(x, y) \\ v(x, y) \end{bmatrix} = \boldsymbol{HU}, \qquad \begin{bmatrix} \varepsilon_x(x, y) \\ \varepsilon_y(x, y) \\ \gamma_{xy}(x, y) \end{bmatrix} = \boldsymbol{EHU} = \boldsymbol{BU}$$

where

$$\boldsymbol{U} = \text{global nodal displacement vector}$$

$$\boldsymbol{H}(x, y) = \begin{bmatrix} \phi_1 & 0 & \phi_2 & 0 & \cdots & \phi_n & 0 \\ 0 & \phi_1 & 0 & \phi_2 & \cdots & 0 & \phi_n \end{bmatrix}$$

$$\boldsymbol{E}(x, y) = \begin{bmatrix} \dfrac{\partial}{\partial x} & 0 \\ 0 & \dfrac{\partial}{\partial y} \\ \dfrac{\partial}{\partial y} & \dfrac{\partial}{\partial x} \end{bmatrix}, \qquad \boldsymbol{\sigma} = \boldsymbol{C\varepsilon} = \boldsymbol{CBU}$$

Then the resulting discretized equations in matrix notations are written as follows:

$$\boldsymbol{KU} = \boldsymbol{F} \tag{18}$$

where

$$\boldsymbol{K} = \int_\Omega \boldsymbol{B}^T \boldsymbol{CB}\, \mathrm{d}v + \frac{1}{\varepsilon} \int_{\Gamma_C} \boldsymbol{H}^T \boldsymbol{n}\, \boldsymbol{n}^T \boldsymbol{H}\, \mathrm{d}s$$

$$\boldsymbol{F} = \int_{\Gamma_F} \boldsymbol{H}^T \boldsymbol{t}\, \mathrm{d}s + \int_{\Gamma_C} \boldsymbol{H}^T \boldsymbol{\sigma}_T\, \mathrm{d}s + \frac{1}{\varepsilon} \int_{\Gamma_C} s\boldsymbol{H}^T \boldsymbol{n}\, \mathrm{d}s$$

Here the following matrix and vector notation are used:

$$\boldsymbol{C} = \begin{bmatrix} C_{11} & C_{12} & C_{13} \\ C_{21} & C_{22} & C_{23} \\ C_{31} & C_{32} & C_{33} \end{bmatrix}, \qquad \boldsymbol{n} = \begin{bmatrix} n_1 \\ n_2 \end{bmatrix}$$

$$\boldsymbol{\sigma}_T = \begin{bmatrix} \sigma_{T_1} \\ \sigma_{T_2} \end{bmatrix}, \qquad \boldsymbol{t} = \begin{bmatrix} t_1 \\ t_2 \end{bmatrix}$$

The integrations on Γ_C are performed only when the value of $u_i n_i - s$ is positive and the reduced integrations are carried out on Γ_C for the stability of the solution.[15]

Algorithm for the Frictional Contact Problem

Step 1. Solve the frictionless contact problem. In this step, the standard Newton–Raphson method is used as a solution procedure. Using the converged solutions, the normal contact stresses are calculated with the following equations:

$$\boldsymbol{\sigma}_N = -(1/\varepsilon)(u_i n_i - s)^+ \boldsymbol{n} \tag{19}$$

Step 2. Calculate the friction force on the contact region:

$$\boldsymbol{\sigma}_T = -\mu |\boldsymbol{\sigma}_N| (\boldsymbol{u}_T/|\boldsymbol{u}_T|)(2/\pi) \tan^{-1}(|\boldsymbol{u}_T|/u_0) \tag{20}$$

The arctangent function is introduced to allow the smooth transition of the frictional stresses from zero to a finite value. Also, the use of this function can fix the problem due to an abrupt sign change of frictional stress in the case of multipin joints. The term u_0 is a positive number, which controls the smoothness of the frictional stress, and has a typical value of 10^{-2}–10^{-3} times $|\boldsymbol{u}_T|$ (Refs. 16 and 17).

Step 3. Solve the frictional contact problem by using the friction force calculated in step 2.

Steps 2 and 3 are repeated until the solution is converged.

Algorithm for the Progressive Failure Analysis

The numerical procedures based on the parallel spring analogy[22] are performed for the failure analysis. Let us assume that the convergence of the solution was achieved at the load level P^{n-1}.

Step 1. Increase the applied load from P^{n-1} to P^n by a small increment ΔP, i.e.,

$$P^n = P^{n-1} + \Delta P$$

Step 2. Solve the frictional contact problem with the current loading state.

Step 3. Calculate in-plane stresses in each ply by coordinate transformation.

Step 4. Assess the failure in each ply using Eqs. (12–15).

Step 5. a) Go to step 1 if no more failure is founded. b) If failure occurs, go to the next steps.

Step 6. Modify material properties by using Eqs. (16) and (17).

Step 7. a) Stop if failure is so much accumulated that no more load can be applied. b) Otherwise, go to step 2.

Numerical Results

Contact Verification

As mentioned in the Introduction, the precise calculation of the stress distribution around the pin hole is very important to predict the failure strengths and the failure modes correctly. To assess the accuracy of the present penalty finite element calculation, the distributions of the contact stress are verified by comparing results with those of previous work.[13,14] The finite element mesh is shown in Fig. 2. Half of the plate is discretized by 534 4-node linear elements with 591 nodes. Finer meshes are used in the vicinity of the hole. Through the numerical results, the mesh system in Fig. 2 is used.

As a verification example, the contact stresses around the hole are compared with the previous results in Fig. 3. The good agreements are shown though all of the contact region is assumed as the slip region. This result can be explained by the fact that most results, except some special ply angles such as $[0]_s$, show the small nonslip region for the small value of friction.[14] Also note that the maximum contact stress is located away from the symmetric line of the plate and the wider contact area is obtained compared with that of the frictionless case.[14]

Comparisons with the Experiment Results

To show the validity of the present formulation, the predictions of the failure strengths and the failure modes are compared with available experimental data and numerical results for graphite/epoxy laminates.[4] The geometric configurations and the ply orientations of the laminated composite plates are listed in Table 1. Each ply orientation is distinguished by Case and geometric configuration by Spec. The failure modes can be identified by the damaged area in the finite element model as shown in Fig. 4.

The comparisons between the present results and the experimental results are shown in Table 2 and Figs. 5 and 6. The friction coefficient is assumed as the value of 0.2, which is the typical value for a steel pin on graphite/epoxy.[25] The failure modes are indicated by the letters T, S, and B, which denote the tension mode, the shear-out mode, and the bearing mode, respectively. As shown in Figs. 5 and 6 and Table 2, the good agreements between the experimental results and the present results are obtained within about a 12% range except for spec 1 and spec 2. Also, the present formulation predicts better results than the method using characteristic curves. But some differences between the experimental results and the present results are shown in the case of spec 1 and spec 2 because the ratio of thickness/width in these specs may be too large for the plane stress assumption. In case 1, it is noticeable that the failure modes are changed according to the existence of the friction. It is well known that the bearing failure is affected critically by the radial stress

Table 1 Dimensions in inches of laminated composite plates (case 1: $[0/45/90]_{3s}$, case 2: $[(0/90)_6]_s$)

		R	*L*	*E*	*W*	*t*:*W*
Case 1	Spec 1	0.0625	5	0.375	0.375	1:3
	Spec 2	0.09365	7	0.375	0.71	1:5.7
	Spec 3	0.25	7	1.5	1.47	1:11.8
	Spec 4	0.25	7	1.5	3.0	1:24
Case 2	Spec 1	0.0625	5	0.375	0.38	1:3.1
	Spec 2	0.09365	7	0.375	0.75	1:6
	Spec 3	0.25	7	1.5	1.5	1:12
	Spec 4	0.25	7	1.5	2.5	1:20

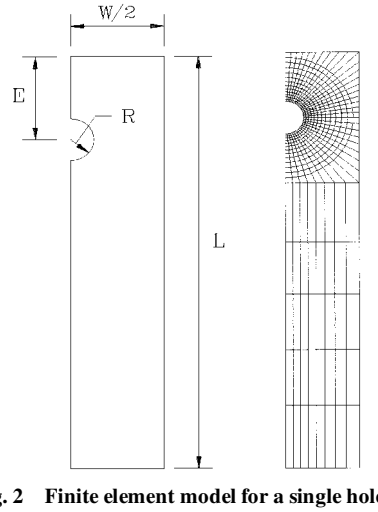

Fig. 2 Finite element model for a single hole.

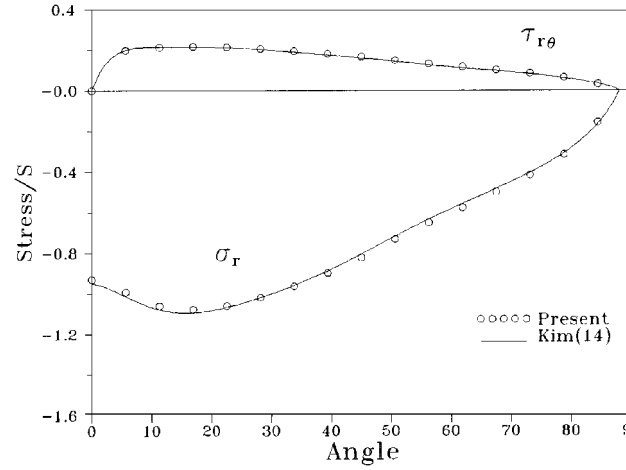

Fig. 3 Comparison of present results with previous results[14] ($[0_2/\pm 45]_s$, $\lambda = 0$).

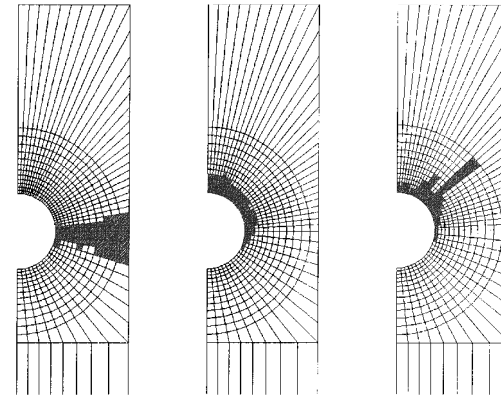

Tension mode **Bearing mode** **Shear-out mode**

Fig. 4 Identification of a failure mode in the finite element model.

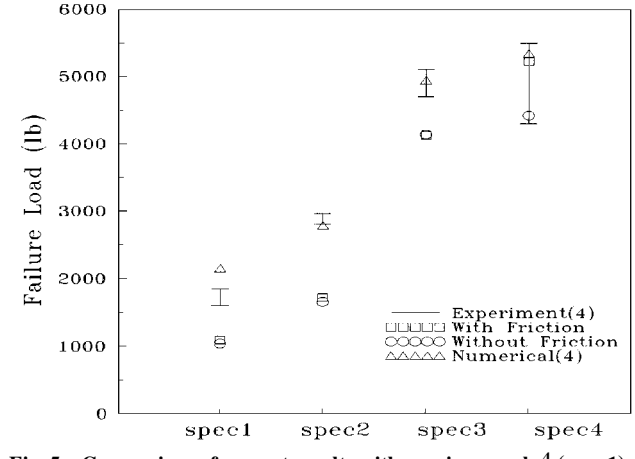

Fig. 5 Comparison of present results with previous works[4] (case 1).

Table 2 Comparisons in pounds with the experimental results[4] (case 1: $[0/45/90]_{3s}$, case 2: $[(0/90)_6]_s$)

		Averaged experimental results		Frictionless		Frictional	
		Strength	Mode	Strength	Mode	Strength	Mode
Case 1	Spec 1	1725	T	1049	T/B	1150	T
	Spec 2	2890	T	1688	B	1789	T
	Spec 3	4920	T	4284	B	4330	T
	Spec 4	4825	B	4933	B	5394	B
Case 2	Spec 1	1392	S/T	1076	S	1112	S
	Spec 2	2150	S/T	1766	S	1721	S
	Spec 3	4875	S/T	4170	S	4393	S/T
	Spec 4	4700	B/S	4524	B	4831	B/S

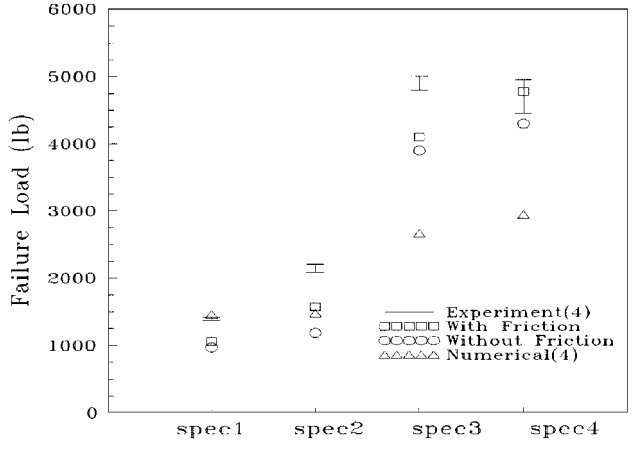

Fig. 6 Comparison of present results with previous works[4] (case 2).

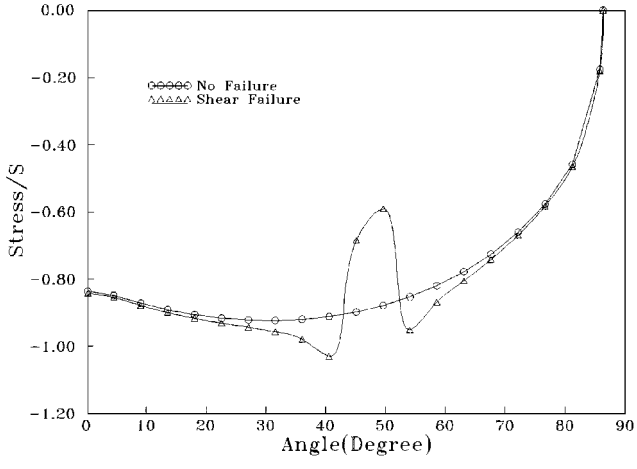

Fig. 7 Variation of contact stress during the shear-out failure process.

distribution around the hole,[26] and the friction changes the radial stress distribution around the hole.[14] Therefore, the frictional effect should be included for the better prediction of the failure modes and the failure strengths in the design of the pin joint structures.

As remarked earlier, the contact stresses vary according to the degree of material degradation. This is shown clearly in Fig. 7, where two normal contact stresses, one before the failure and the other during the failure process, are shown when the typical shear-out mode occurs. It can be seen that, once a portion of material is degraded, the contact stress on this portion is reduced and the stress concentrations are found at the near edges of this portion. This phenomenon changes the local load path in the pin–hole area. Therefore, it can be stated that the failure analysis considering varying contact stresses properly is also necessary for the better prediction of the failure strengths and the failure modes.

Parametric Study

Next, the effects of geometric factors and of the clearance between the pin and the hole on the failure strengths and the failure modes

Table 3 Reference dimensions in inches for the parametric study

L	7
W	1
E	1
$D = 2R$	0.25
t	0.1

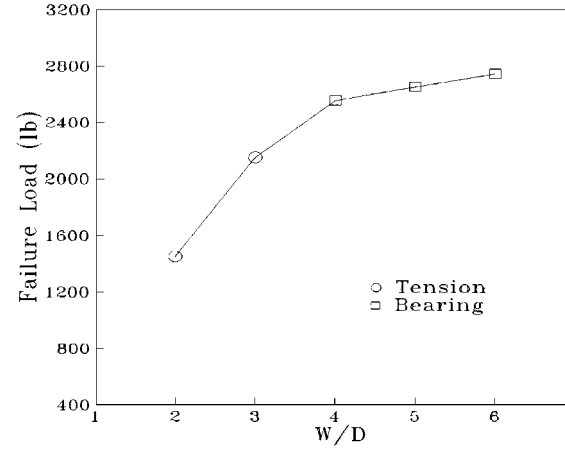

Fig. 8 Effect of *W/D* (case 1).

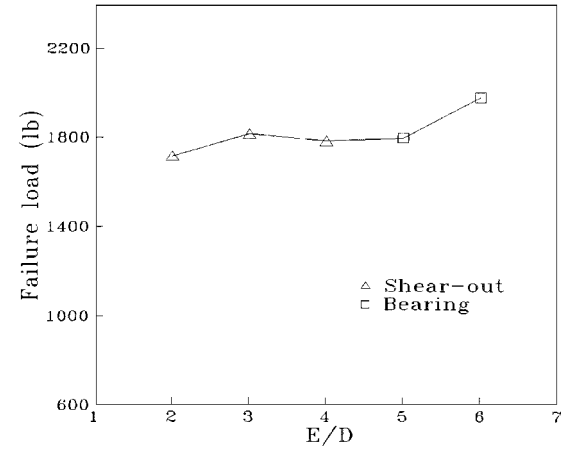

Fig. 9 Effect of *E/D* (case 2).

are studied for the two laminates used earlier (case 1: $[0/\pm 45/90]_{3s}$ and case 2: $[(0/90)_6]_s$). The width of the plate and the distance from the upper edge of the plate to the hole center are taken as geometric factors. Each geometric factor is nondimensionalized by the hole diameter D. The reference values of each dimension are listed in Table 3. The friction coefficient has a value of 0.2.

First, the effects of the geometry are examined and the results are shown in Figs. 8 and 9. In Fig. 8, the width of the plate (W/D) is taken as a geometric factor. In case 1, the failure strengths increase by a factor of 2 as the plate becomes wider. It can be seen that failure modes change from tension mode to bearing mode as the plate becomes wider. In case 2, although all of the results are not shown in the paper, it is noted that the increase of the failure strength is significant and the failure strengths increase by three times as the plate becomes wider. But the failure modes do not change for the variation of W/D. Second, the effects of the distance from the edge of the plate to the hole center (E/D) are analyzed in Fig. 9 for case 2. For both of the laminates, E/D has little effect on the failure strengths, unlike W/D from Fig. 8 and our computational experience. It is an interesting fact that the failure modes change to bearing mode for both of the cases as E/D becomes bigger. This result is explained by the fact that the location of the maximum contact stress moves toward the symmetric line of the plate as E/D becomes bigger.[27] Finally, the effects of clearance between the pin and the hole are

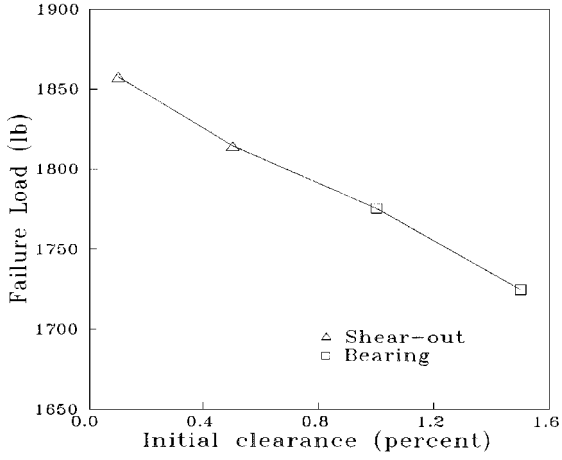

Fig. 10 Effect of initial clearance λ (case 2).

studied in Fig. 10. For both of the cases, it is noted that the failure strengths decrease when the clearance increases, although we show only the result of case 2. The failure mode changes from shear-out mode to bearing mode in case 2, whereas there is no transition of failure mode in case 1. The results can be explained by the fact that as the clearances are bigger, the maximum contact stress increases and the contact area becomes smaller.[27] From the results, it can be stated that the geometric factors and clearances have important roles in determining the failure strengths and the calculation of the failure modes, and the calculations of the precise distribution of contact stress are needed to identify the failure characteristics correctly.

Conclusions

In this paper, the progressive failure analysis of pin-loaded laminated composite plates is performed to predict the failure strengths and the failure modes. To solve the contact problem between pin and hole, the penalty finite element method is used. As the failure criterion, Hashin's criterion, which can treat the fiber mode and the matrix mode failures separately, is used. The computed contact stresses by the present formulation results are compared with previous works and agree well with both the frictionless and frictional cases. Also, the predictions of the failure strengths and the failure modes are compared with the available experimental data and show the excellent agreement within about a 12% range. Through the parametric study considering geometries and clearance, the importance of these factors on the failure characteristics of the pin-loaded laminated composite plate is identified. These factors change the failure strengths and the failure modes significantly.

It can be concluded that the present formulation based on the rigorous mechanical foundations is a reasonable and an efficient tool for predicting the failure characteristics of the pin-loaded laminated composite plate. As extended work of the present formulation, the three-dimensional analyses, which consider the nonlinear shear stress–strain relations,[27] the clamping forces, and the delamination with the local buckling due to the high through-the-thickness stress (σ_{zz}) on the loaded side of the hole in the case of bearing failure, need to be done and will be presented in a forthcoming paper.

References

[1]Waszczak, J. P., and Cruse, T. A., "Failure Mode and Strength Predictions of Anisotropic Bolt Bearing Specimens," *Journal of Composite Materials*, Vol. 5, 1971, pp. 421–425.

[2]Oplinger, D. W., and Gandhi, K. R., "Analytic Studies of Structural Performance in Mechanically Fastened Fiber-Reinforced Plates," Army Materials and Mechanics Research Center, AMMRC-MS-74-8, Watertown, MA, 1974.

[3]Tsai, M. Y., and Morton, J., "Stress and Failure Analysis of a Pin-Loaded Composite Plate: An Experimental Study," *Journal of Composite Materials*, Vol. 24, 1990, pp. 1101–1121.

[4]Chang, F. K., Scott, R. A., and Springer, G. S., "Failure of Composite Laminates Containing Pin Loaded Holes—Method of Solution," *Journal of Composite Materials*, Vol. 18, 1984, pp. 255–278.

[5]Chang, F. K., Scott, R. A., and Springer, G. S., "Design of Composite Laminates Containing Pin Loaded Holes," *Journal of Composite Materials*, Vol. 18, 1984, pp. 279–289.

[6]Chang, F. K., "The Effect of Pin Load Distribution on the Strength of Pin Loaded Holes in Laminated Composites," *Journal of Composite Materials*, Vol. 20, 1986, pp. 401–408.

[7]Chang, F. K., and Chang, K. Y., "Post-Failure Analysis of Bolted Composite Joints in Tension or Shear-Out Mode Failure," *Journal of Composite Materials*, Vol. 21, 1987, pp. 809–833.

[8]Oplinger, D. W., Gandhi, W., and Gandhi, K. R., "Stress in Mechanically Fastened Orthotropic Laminates," 2nd Conf. of Fibrous Composites in Flight Vehicle Design, 1974, pp. 813–841.

[9]Wong, C. M., and Matthews, F. L., "A Finite-Element Analysis of Single and Two-Hole Bolted Joints in Orthotropic Materials," *Journal of Composite Materials*, Vol. 15, 1981, pp. 481–491.

[10]Soni, S. R., "Failure Analysis of Composite Laminates with a Fastened Hole," *Journal of Composite Materials*, Vol. 15, 1981, pp. 145–164.

[11]Agarwal, B. L., "Static Strength Prediction of Bolted Joint in Composite Material," *AIAA Journal*, Vol. 18, No. 11, 1980, pp. 1371–1375.

[12]De Jong, T., "The Influence of Friction on the Theoretical Strength of Pin-Loaded Holes in Orthotropic Plates," Dept. of Aerospace Engineering, Delft Univ. of Technology, Rept. LR-350, Delft, The Netherlands, 1982.

[13]Kim, S. J., and Kim, J. H., "Finite Element Analysis of Laminated Composites with Contact Constraint by Extended Interior Penalty methods," *International Journal for Numerical Methods in Engineering*, Vol. 36, No. 20, 1993, pp. 3421–3439.

[14]Kim, S. J., and Kim, J. H., "Finite Element Analysis of Laminated Composite Plates with Multi Pin Joints Considering Friction," *Computer and Structures*, Vol. 55, No. 3, 1995, pp. 507–514.

[15]Oden, J. T., Kikuchi, N., and Song, Y. J., "Reduced Integration and Exterior Penalty Methods for Finite Element Approximations of Contact Problems in Incompressible Linear Elasticity," Univ. of Texas, TICOM Rept. 80-2, Austin, TX, 1980.

[16]Kobayashi, S., Oh, S. I., and Atlan, T., *Metal Forming and the Finite-Element Method*, Oxford Univ. Press, Oxford, England, UK, 1989, pp. 86, 87.

[17]Kim, S. J., Kim, J. H., Kim, W. D., and Jung, S. N., "A Numerical Simulation of Damage Propagation During Metal Forming Process," *Proceedings of 1st Pacific Conference on Manufacturing*, Indonesia, 1994, pp. 198–205.

[18]Hashin, Z., "Failure Criteria for Uniaxial Fiber Composites," *Journal of Applied Mechanics*, Vol. 47, 1980, pp. 329–334.

[19]Lee, J. D., "Three Dimensional Finite Element Analysis of Damage Accumulation in Composite Laminates," *Computers and Structures*, Vol. 15, 1982, pp. 41–47.

[20]Duvaut, G., and Lions, J. L., *Inequalities in Mechanics and Physics*, Springer, Berlin, 1976.

[21]Campos, L. T., Oden, J. T., and Kikuchi, N., "A Numerical Analysis of a Class of Contact Problems with Friction," *Computer Methods in Applied Mechanics and Engineering*, Vol. 34, 1982, pp. 821–845.

[22]Jones, R. M., *Mechanics of Composite Materials*, Scripta, Washington, DC, 1975, pp. 190–192.

[23]Tsai, S. W., "Strength Characteristics of Composite Materials," NACA CR-224, April 1965.

[24]Tsai, S. W., and Wu, E. M., "Failure Theory for Filamentary Composites," *Composite Materials, Testing and Design*, American Society of Testing and Materials, STP 460, Philadelphia, PA, 1970, pp. 336–351.

[25]Hyer, M. W., Klang, E. C., and Cooper, D. E., "The Effect of Pin Elasticity, Clearance and Friction on the Stresses in a Pin-Loaded Orthotropic Plate," *Journal of Composite Materials*, Vol. 21, 1987, pp. 190–206.

[26]Matthews, F. L., *Joining Fibre-Reinforced Plastics*, Elsevier Applied Science, London, 1987, pp. 16–21, Chap. 2.

[27]Kim, S. J., and Kim, J. H., "The Effects of Geometries, Clearances and Frictions on the Composite Multi-Pin Joints," *AIAA Journal*, Vol. 34, No. 4, 1996, pp. 862–864.

R. K. Kapania
Associate Editor